Journal of Physics: Conference Series **1445** (2020) 012005 doi:10.1088/1742-6596/1445/1/012005

A Computational Theory Study of Surface Plasmon Resonance (SPR) Porcine Gelatine Detected Sensor based-on Fe_3O_4 Nanoparticle—CNT with ATR Method in Kretschmann Configuration

Maulina Lutfiyah[1], **Wahyu Aji Eko Prabowo**[2,3], **Asih Melati**[1,*]

[1]Department of Physics, Faculty of Science and Technology, Universitas Islam Negeri Sunan Kalijaga, Yogyakarta 55281, Indonesia
[2]Research Center for Quantum Engineering Design, Faculty of Science and Technology, Universitas Airlangga, Surabaya 60115, Indonesia
[3]Informatics Engineering Department, Faculty of Computer Science, Universitas Dian Nuswantoro, Semarang 50131, Indonesia

E-mail: asih.melati@gmail.com

Abstract. Accurate biomolecular detection can be performed through the Surface Plasmon Resonance (SPR) phenomenon. This study was conducted to simulate the effect of the addition of Fe_3O_4 nanoparticle and Carbon Nanotube (CNT) in the Kretschmann and Otto configurations using porcine detection sensors. This study employs the equation of reflectance for the investigations of SPR properties (i.e. SPR angle and reflectance value) using Matlab software version 7.12.0. This research was used ATR method with Kretschmann configuration, He-Ne laser on wavelength 632.8 nm, semi-circle prism type BK7 and metal layer of gold nanoparticles. The results of this research can be used in the detection of porcine gelatine by Kretschmann configurations. The best thickness of the gold layer and Fe_3O_4 layer are 50 nm and 0.05 nm. Moreover, the thickness of SWCNT used is 15 nm. The applied SWCNT is more effective than MWCNT on porcine detection. The SWCNT material also proved to be better used in SPR systems.

Keywords: CNT, Fe_3O_4 Nanoparticle, Porcine Gelatine, SPR

1. Introduction

The sensing halal food methodology by religion of fair in Indonesia becomes primary topic research of Islamic state university in Indonesia. Surface Plasmon Resonance (SPR) equipment system assist the technological development, such as in health, medicine, or industry applications. Biosensor system on SPR is expected to be used as a detection sensor of halal food product. In Indonesia issue related halal food content are important, for example porcine gelatine. The content of porcine in a processed product such as gelatine is difficult to know directly. Therefore, it need a tool that is able to detect the presence of porcine content in a product. The SPR-based biosensor was developed as a detector of meat and porcine gelatine quantitatively in Gadjah Mada university [1]. The addition of Fe_3O_4 magnetic nanoparticles to SPR systems can improve SPR responses, even though without using ligands to mobilize proteins [2]. The biological molecules interaction in the sensing medium in example porcine are detected by observing the refractive index changes of the sensor region. Coating material thin film system on prism - Fe_3O_4 and Carbon Nanotubes (CNT) can also be used in SPR-based sensor systems. Nowadays, CNTs have been widely used in various optoelectronic devices, super capacitors, and various types of sensors. By combining Fe_3O_4 nanoparticle and CNT is expected to improve the detection of product content using SPR equipment. Graphene has been proposed for the enhancement of sensitivity [3]. Computational study has been widely applied in many areas including

health and medicine. For example, to analyze customer's health behaviour [4] and to design drugs [5]. In this paper, we utilize the computational based study to simulate the detection of porcine gelatine using Fe_3O_4 nanoparticle and CNT which implemented in SPR equipment.

2. Computational Details

2.1. Optical Phenomenon in Medium

The propagation of electromagnetic wave radiation within the material has been described in Maxwell's equations as follows:

$$\nabla \bullet \vec{D} = \rho \tag{2.1}$$

$$\nabla \bullet \vec{B} = 0 \tag{2.2}$$

$$\nabla \times \vec{E} = -\frac{\partial \vec{B}}{\partial t} \tag{2.3}$$

$$\nabla \times \vec{H} = \vec{J} + \frac{\partial \vec{D}}{\partial t} \tag{2.4}$$

∇ is vector operator that divine as $\nabla = \hat{i}\frac{\partial}{\partial x} + \hat{j}\frac{\partial}{\partial y} + \hat{k}\frac{\partial}{\partial z}$. Whereas $\vec{D}$ is the dielectric flux density, $\vec{B}$ is the magnetic flux density, $\vec{E}$ is the electric field, and $\vec{H}$ is the magnetic field [6].

Electromagnetic waves are transverse waves and have two polarization components. On *p* wave (polarized p, TM = transverse magnetic), the magnetic field component is perpendicular to the incident plane. In that case, *p* wave has *E* component of the X and Z-axis direction [7, 8].

$$n_1\left(E_p - R_p\right) = n_2 T_p \tag{2.5}$$

If *r* is defined as the reflection amplitude coefficient, then

$$r_p = \frac{R_p}{E_p} \tag{2.6}$$

$$\left(1 - r_p\right)\cos\theta = t_p \cos\theta'' \tag{2.7}$$

$$n_1\left(1 + r_p\right) = n_2 t_p \tag{2.8}$$

Reflectance (R) can be written as a comparison of reflectivity to the incident light power [6],

$$R = \frac{I'A\cos\theta''}{IA\cos\theta''} = \frac{I'}{I} = \frac{n_1 R^2/\left(2c\mu_0\right)}{n_1 E^2/\left(2c\mu_0\right)} = r^2 \tag{2.9}$$

2.2. Surface Plasmon Resonance (SPR)

Surface Plasmon Resonance (SPR) is a physical process that occurs when polarized light shoots/ irradiates a metal film under internal reflection conditions. The SPR effect is sensitive to the binding of analyte because the associated increase in mass causes a proportional increase in refractive index, which is observed as a shift in the resonance angle. A flow injection analysis configuration is commonly employed in which the analyte of interest, solvated in a buffer solution, is transported across the sensing surface, where it interacts with the immobilized biomolecule [9, 10]. The SP wave vector is determined only by the dielectric constant of the metal and its dielectric material, given by the relationship with ε_d and ε_m, so we can also write the following equation,

$$K_{sp} = \frac{\omega}{c}\sqrt{\frac{\varepsilon_d \varepsilon_m}{\varepsilon_d + \varepsilon_m}} = \left(\frac{2\pi}{\lambda}\right)\sqrt{\frac{\varepsilon_d \varepsilon_m}{\varepsilon_d + \varepsilon_m}} \tag{2.11}$$

The reflectance intensity for 3 layer system (prism, metal, and medium) in the Kretschmann configuration based on the Fresnel formula for the p-polarization is shown by the following equation,

$$R = \left| \frac{r_{pr1} + r_{12} e^{2iK_{zidi}}}{1 + r_{pr1} r_{12} e^{2iK_{zidi}}} \right|^2 \tag{2.12}$$

$$r_{ij} = \left(\frac{K_{zi}}{\varepsilon_i} - \frac{K_{zj}}{\varepsilon_j} \right) \Big/ \left(\frac{K_{zi}}{\varepsilon_i} + \frac{K_{zj}}{\varepsilon_j} \right) \tag{2.13}$$

$$K_{zi} = \frac{2\pi}{\lambda} \left(\varepsilon_i - n_p^2 \sin^2 \theta \right)^{\frac{1}{2}} \tag{2.14}$$

With r_{ij} shown the reflectance coefficients at the intermediate i and medium interfaces, K_{zi} denotes the perpendicular surface wave vector components, in and ε_i (i = 1, 2, 3) are the thickness and the dielectric constant of the medium to -i [7, 11, 12].

2.3. Materials and Modelling

To understanding the surface plasmon excitation can use the Attenuated Total Reflection (ATR) methods. There are two configurations of the ATR methods, Kretschmann and Otto configurations, respectively [13].

The Kretschmann configuration is composed of a prism with a n_p refractive index with a metal-dielectric surface comprising a thin metal layer with ε_m and q thickness, and semi-infinite dielectrics with n_d refractive index ($n_d < n_p$). In the Kretschmann configuration, the metallic layer is in direct contact with the prism while the dielectric layer covers the metal layer [10]. This configuration is more able to use in experimental research. So this study is using Kretschmann configuration with Matlab 7.12.0 software and winspall application. The metal material that used are gold nanoparticles, dielectric material is Fe_3O_4, CNT, and porcine gelatine.

Magnetic nanoparticles are magnetic materials of nanometer size. The Fe_3O_4 magnetic nanoparticles can be used as a Surface Plasmon Resonance (SPR) based biosensor. The Fe_3O_4 nanoparticles may be super paramagnetic. These properties make Fe_3O_4 able to interact with biomolecules. Some property values of Fe_3O_4 when subjected to He-Ne laser light with a wavelength of 632.8 nm have a refractive index (n = 2.162 + 1.178 i) [14].

Carbon Nanotube (CNT) is one of carbon structure that is shaped like a cylinder with a diameter in nanometer order. CNTs have some emphasize useful optical or feeding properties. The optical properties of MWCNT and SWCNT have some differences. Based on its chemical structure, MWCNT has optical properties similar to graphite, whereas SWCNT is similar to carbon.

Gelatine is a protein derivative of collagen fibers present in the skin, bones, and cartilage. The gelatine of each animal can be distinguished by its amino acid content and chemical structure. Physically, the difference of amino acid content can be known through the difference of refractive index. The index of refractive porcine gelatine through SPR phenomena with wavelength of 632.8 nm laser light is 1.3351 [1].

This study are determined using computer with Windows 7 operating system that has Matlab 7.12.0 software with license number 161052 and winspall application version 3.02.

3. Results and Discussion

This research was conducted theoretical computational-based. SPR modelling is done by ATR (Attenuated Total Reflection) method. Before the prism was coated with metal material and object identification material, simulations are first made to know the shape of the SPR curve when the prism is empty and look for the critical angle of the prism. Figure 1 shows the simulation result of the relationship between reflectance to the incident angle when the prism is empty.

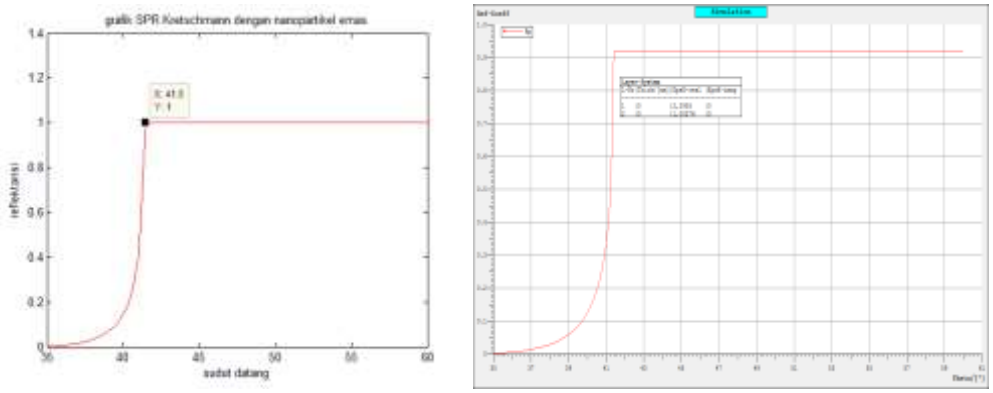

Figure 1. (Left) The reflectance graph of the incident angle when the prism is empty using Matlab 7.12.0 and (right) using Winspall 3.02

The simulation is determined using prism BK7 with refractive index of 1.5151. The results obtained using Matlab 7.12.0 software are similar to those of the Winspall 3.02 application. Based on the result, it is known that when the empty prism increases the value of reflectance before the total reflection or TIR (Total Internal Reflection). TIR occurs when the reflectance value is 1 at 41.5°. This angle is called the critical angle, which means that the refraction of the incident light comes at 90°. After the TIR the rays continue to reflect perfectly. In this system, there is no SPR due to the absence of metal material so there is no surface plasmon wave.

3.1. 3 layers system (prism, gold, air)

$$R = \left| r_{pr12} \right|^2 = \left| \frac{r_{pr1} + r_{12} e^{2iK_{z1}d_1}}{1 + r_{pr1} r_{12} e^{2iK_{z1}d_1}} \right|^2 \tag{3.1}$$

$$r_{pr1} = \frac{\left(\cos\theta / n_{pr}\right) - \left(\varepsilon_1 - n_{pr}^2 \sin^2\theta\right)^{1/2} / \varepsilon_1}{\left(\cos\theta / n_{pr}\right) + \left(\varepsilon_1 - n_{pr}^2 \sin^2\theta\right)^{1/2} / \varepsilon_1} \tag{3.2}$$

$$r_{12} = \frac{\left(\varepsilon_1 - n_{pr}^2 \sin^2\theta\right)^{1/2} / \varepsilon_1 - \left(\varepsilon_2 - n_{pr}^2 \sin^2\theta\right)^{1/2} / \varepsilon_2}{\left(\varepsilon_1 - n_{pr}^2 \sin^2\theta\right)^{1/2} / \varepsilon_1 + \left(\varepsilon_2 - n_{pr}^2 \sin^2\theta\right)^{1/2} / \varepsilon_2} \tag{3.3}$$

$$K_{z1} d_1 = \frac{\omega}{c} d_1 \left(\varepsilon_1 - n_{pr}^2 \sin^2\theta\right)^{1/2} \tag{3.4}$$

The graph shows that with the addition of gold nanoparticles, there is a decrease in the value of reflectance (attenuation). Attenuation occurs when the angle is greater than the critical angle. This suggests that the addition of gold coatings can lead to surface plasmon waves. Reflectance value at 50 nm gold thickness is seen as smallest. Figure 2 shows that there is an increase in the reflectance before the total reflectance, then the reflectance decrease occurs as it approaches the total reflection. This indicates a resonance occurring on the surface between gold with a prism and laser beam waves. The decrease in the reflectance value indicates the level of light absorption. A emphasize large drop of reflectance occurs at a gold thickness of 50 nm.

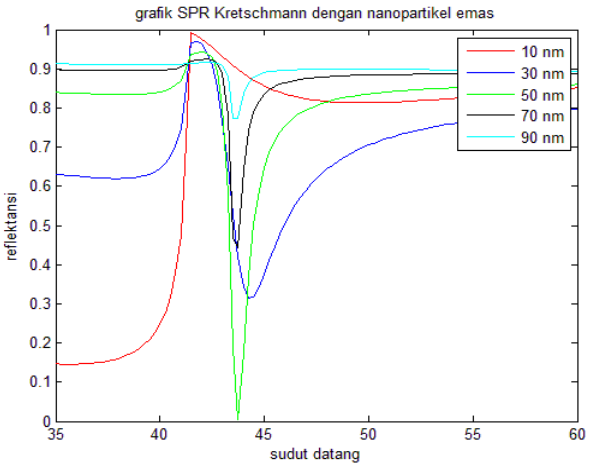

Figure 2. Kretschmann configuration SPR graph on 3 layer system with gold thickness variation

3.2. *4 layers system (prism, gold, Fe_3O_4, air)*

$$R = \left|r_{pr123}\right|^2 = \left|\frac{r_{pr1} + r_{123}e^{2iK_{z1}d_1}}{1 + r_{pr1}r_{123}e^{2iK_{z1}d_1}}\right|^2 \tag{3.5}$$

$$r_{23} = \frac{\left(\varepsilon_2 - n_{pr}^2 \sin^2\theta\right)^{1/2}/\varepsilon_2 - \left(\varepsilon_3 - n_{pr}^2 \sin^2\theta\right)^{1/2}/\varepsilon_3}{\left(\varepsilon_2 - n_{pr}^2 \sin^2\theta\right)^{1/2}/\varepsilon_2 + \left(\varepsilon_3 - n_{pr}^2 \sin^2\theta\right)^{1/2}/\varepsilon_3} \tag{3.6}$$

$$r_{123} = \frac{r_{12} + r_{23}e^{2iK_{z2}d_2}}{1 + r_{12}r_{23}e^{2iK_{z2}d_2}} \tag{3.7}$$

$$K_{z2}d_2 = \frac{\omega}{c}d_2\left(\varepsilon_2 - n_{pr}^2 \sin^2\theta\right)^{1/2} \tag{3.8}$$

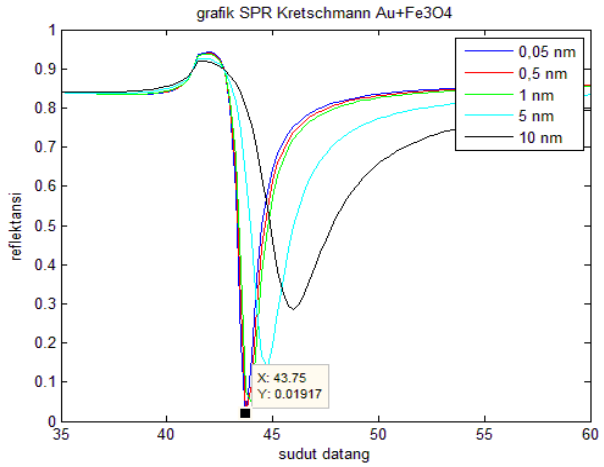

Figure 3. Kretschmann configuration SPR graph on 4 layer system with Fe_3O_4 thickness variation

The four-layer system created is a prism, 50 nm gold nanoparticles, Fe_3O_4 nanoparticles, and air. The addition of 0.05 nm Fe_3O_4 nanoparticles did not cause a SPR angular shift but decreased the reflectance value to 0.004016. However, in the addition of nanoparticles with larger thickness causes

the SPR angle to become larger (there is a shift curve to the right). Figure 3 shows the Kretschmann configuration SPR graph on 4 layer system with Fe_3O_4 thickness variation

3.3.5 layers system (prism, gold, Fe_3O_4, CNT, air)

3.3.1. 5 layers system (prism, gold, Fe3O4, MWCNT, air)

$$R = \left|r_{pr1234}\right|^2 = \left|\frac{r_{pr1} + r_{1234}e^{2iK_{z1}d_1}}{1 + r_{pr1}r_{1234}e^{2iK_{z1}d_1}}\right|^2 \tag{3.9}$$

$$r_{34} = \frac{\left(\varepsilon_3 - n_{pr}^2\sin^2\theta\right)^{1/2}/\varepsilon_3 - \left(\varepsilon_4 - n_{pr}^2\sin^2\theta\right)^{1/2}/\varepsilon_4}{\left(\varepsilon_3 - n_{pr}^2\sin^2\theta\right)^{1/2}/\varepsilon_3 + \left(\varepsilon_4 - n_{pr}^2\sin^2\theta\right)^{1/2}/\varepsilon_4} \tag{3.10}$$

$$r_{234} = \frac{r_{23} + r_{34}e^{2iK_{z3}d_3}}{1 + r_{23}r_{34}e^{2iK_{z3}d_3}} \tag{3.11}$$

$$r_{1234} = \frac{r_{12} + r_{234}e^{2iK_{z2}d_2}}{1 + r_{12}r_{234}e^{2iK_{z2}d_2}} \tag{3.12}$$

$$K_{z3}d_3 = \frac{\omega}{c}d_3\left(\varepsilon_3 - n_{pr}^2\sin^2\theta\right)^{1/2} \tag{3.13}$$

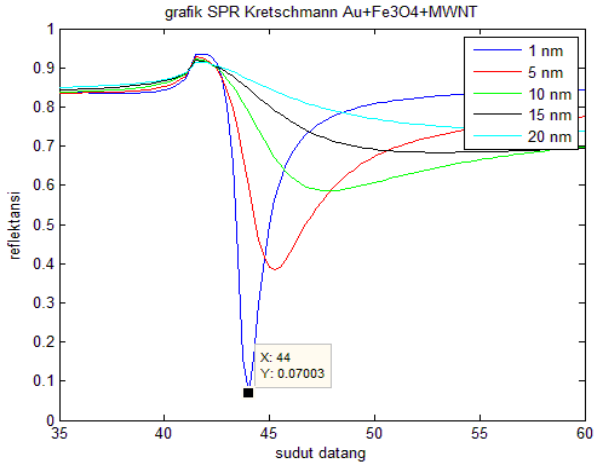

Figure 4. Kretschmann configuration SPR graph with varying thickness of MWCNT

Figure 4 shows Kretschmann configuration SPR graph with a thickness of 50 nm and the thickness of Fe_3O_4 is 0.05 nm while the thickness of MWCNT is varied. At the thickness of MWCNT 1 nm, 5 nm, and 10 nm SPR angle and reflectance becomes larger. However, at 15 nm and 20 nm thickness no SPR occurs. At a thickness of 1 nm the reflectance value is emphasize large when compared with systems that only use the addition of gold and Fe_3O_4 layers. However, in this system there is no decrease in reflectance value. Therefore, the addition of MWCNT in this system is less than optimal, especially when used in the detection of biomolecules.

3.3.2. 5 layers system (prism, gold, Fe3O4, SWCNT, air)

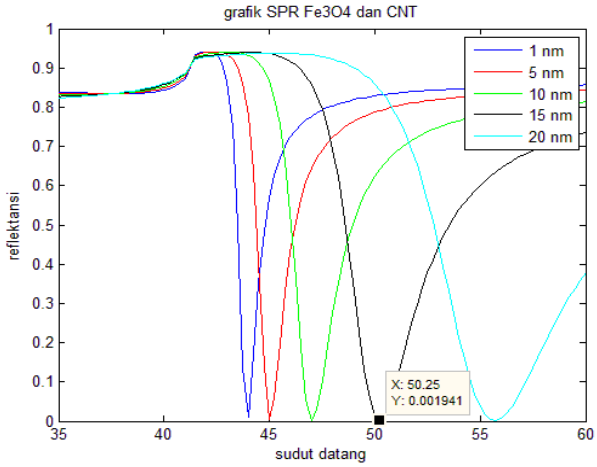

Figure 5. Graph of Kretschmann SPR configuration on 5 layer system with SWCNT thickness variation

Figure 5 shows Kretschmann configuration SPR graph on SWCNT thickness variation is made similar to the MWCNT thickness variation. The results obtained are the thicker layer SWCNT shifting angle SPR with greater and smaller reflectance value. This indicates that the addition of SWCNT increase the absorption of light. From these results it can be seen that the use of SWCNT is better than MWCNT because it is more sensitive because it has smaller reflectance values and larger SPR angles.

3.4. 6 layers system (prism, gold, Fe_3O_4, CNT, gelatine, air)

$$R = \left|r_{pr12345}\right|^2 = \left|\frac{r_{pr1} + r_{12345}e^{2iK_{z1}d_1}}{1 + r_{pr1}r_{12345}e^{2iK_{z1}d_1}}\right|^2 \tag{3.14}$$

$$r_{45} = \frac{\left(\varepsilon_4 - n_{pr}^2 \sin^2\theta\right)^{1/2}/\varepsilon_4 - \left(\varepsilon_5 - n_{pr}^2 \sin^2\theta\right)^{1/2}/\varepsilon_5}{\left(\varepsilon_4 - n_{pr}^2 \sin^2\theta\right)^{1/2}/\varepsilon_4 + \left(\varepsilon_5 - n_{pr}^2 \sin^2\theta\right)^{1/2}/\varepsilon_5} \tag{3.15}$$

$$r_{345} = \frac{r_{34} + r_{45}e^{2iK_{z4}d_4}}{1 + r_{34}r_{45}e^{2iK_{z4}d_4}} \tag{3.16}$$

$$r_{2345} = \frac{r_{23} + r_{345}e^{2iK_{z3}d_3}}{1 + r_{23}r_{345}e^{2iK_{z3}d_3}} \tag{3.17}$$

$$r_{12345} = \frac{r_{12} + r_{2345}e^{2iK_{z2}d_2}}{1 + r_{12}r_{2345}e^{2iK_{z2}d_2}} \tag{3.18}$$

$$K_{z4}d_4 = \frac{\omega}{c}d_4\left(\varepsilon_4 - n_{pr}^2 \sin^2\theta\right)^{1/2} \tag{3.19}$$

The biosensor system built in this study is the addition of Fe_3O_4 and CNT nanoparticles. Optical properties of SWCNT more support on biosensor on SPR systems. The addition of 0.05 nm Fe_3O_4 nanoparticles and 15 nm SWCNT in the 6-layers system made indicated a right-angle SPR shift of 0.25 and a substantial increase of reflectance value 0.01508. Figure 6 shows the SPR angle shift to the right and the increasing reflectance value indicate the presence of detected biomolecules porcine gelatine. A large increase in reflectance value indicates great biosensor sensitivity as well.

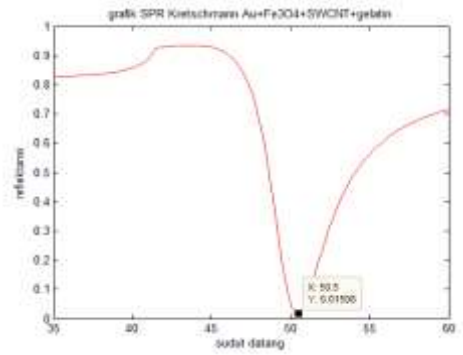

Figure 6. SPR graphs with the addition of Fe_3O_4 and CNT nanoparticles with Kretschmann configuration as porcine gelatin detection sensors

4. Conclusion

Based on the results, it showed that in the Kretschmann configuration, there is a decreasing trend reflectance value by adding 0.05 nm Fe_3O_4 nanoparticles although do not shifting the SPR angle, but after the addition of SWCNT nanoparticles, the SPR angle shifts to the right and the reflectance also decreases. The use of porcine gelatine layer on the system made shows that there is a shift of SPR angle and increase of reflectance value, so that the system made supported to detect the presence of porcine gelatine biomolecules.

References

[1] Wardani D P *et al* 2015 *SPIEE Proceedings*, Prague
[2] Lee K S *et al* 2011 *Journal of Material Chemistry* vol. **21**, pp. 5156-5162
[3] Zeng S, Hu S, Xia J, Anderson T 2015 *Sensor Actuators B Chem.* Vol **207**, pp. 801-810
[4] Puspitasari I 2017 *IEEE* 15th International Conference on Software Engineering Research, Management and Applications (SERA) The 7th-9th of June 2017 London
[5] Disney M D and Angelbello A J 2016 *Acc. Chem. Res.* **49** 12 2698-2704
[6] Wangness, Roald K 1979 *Electromagnetic Field*, John Willey and Sons, Inc. Canada.
[7] Yamamoto M 2008 *Surface Plasmon Resonance (SPR) Theory: Tutorial*, Kyoto University Press, Nishikyo-ku, Japan
[8] Sarid D, Challener W 2010 *Modern Introduction to Surface Plasmons: Theory, Mathematica Modeling, and Applications*, Cambridge University Press, New York
[9] Homola J 2006 *Surface Plasmon Resonance Based Sensors*, Springer, Berlin
[10] Singh P 2014 *Nanotechnology Science and Technology: Surface Plasmon Resonance*, Nova Science Publishers Inc. New York
[11] Jahanshahi P and Rafiq F 2015 *Medical and Bio engineering Journal*, vol. **4**, pp. 2
[12] Mayasari R D *et al* 2012 *Prosiding Pertemuan Ilmiah XXVI HFI Jateng dan DIY*
[13] Schasfoort R B M and Tudos A J 2008 *Handbook of Surface Plasmon Resonance*, The Royal Society of Chemistry, Cambridge
[14] Sari R and Abraham K 2012 *Prosiding Pertemuan Ilmiah XXVI HFI Jateng dan DIY*

Acknowledgments

We woud like grateful to The Computational Laboratory, Department of Physics, Universitas Islam Negeri Sunan Kalijaga, Yogyakarta for computer facility and For the funds of research LPPM UIN Sunan Kalijaga in 2017.